ADVANCES IN ATMOSPHERIC SCIENCES, VOL. 34, DECEMBER 2017, 1415–1425

• **Original Paper** •

Variation in Brewer–Dobson Circulation During Three Sudden Stratospheric Major Warming Events in the 2000s

Mengchu TAO[1,2], Yi LIU[1], and Yuli ZHANG*[1]

[1] *Institute of Atmospheric Physics, Chinese Academy of Sciences, Beijing* 100029*, China*
[2] *University of Chinese Academy of Sciences, Beijing* 100049*, China*

(Received 18 December 2016, revised 3 June 2017, accepted 5 June 2017)

ABSTRACT

As the strongest subseasonal atmospheric variability during boreal winter, three remarkable sudden stratospheric major warming (SSW) events in the 2000s are investigated in terms of the Brewer–Dobson circulation (BDC) response. Our study shows that the changes of cross-isentropic velocity during the SSWs are not only confined to the polar region, but also extend to the whole Northern Hemisphere: enhanced descent in the polar region, as well as enhanced ascent in the tropics. When the acceleration of the deep branch of the BDC descends to the middle stratosphere, its strength rapidly decreases over a period of one to two weeks. The acceleration of the deep branch of the BDC is driven by the enhanced planetary wave activity in the mid-to-high-latitude stratosphere. Different from the rapid response of the deep branch of the BDC, tropical upwelling in the lower stratosphere accelerates up to 20%–40% compared with the climatology, 20–30 days after the onset of the SSWs, and the acceleration lasts for one to three months. The enhancement of tropical upwelling is associated with the large-scale wave-breaking in the subtropics interacting with the midlatitude and tropical Quasi-Biennial Oscillation–related mean flow.

Key words: sudden stratospheric major warming, Brewer–Dobson circulation, subtropical wave

Citation: Tao, M. C., Y. Liu, and Y. L. Zhang, 2017: Variation in Brewer–Dobson circulation during three sudden stratospheric major warming events in the 2000s. *Adv. Atmos. Sci.*, **34**(12),1415–1425,https://doi.org/10.1007/s00376-017-6321-1.

1. Introduction

Sudden stratospheric major warming (SSW), characterized by a rapid temperature rise and strong wind disturbance in the polar stratosphere, has been identified as the most pronounced subseasonal dynamical phenomenon in the boreal winter atmosphere. Among the various definitions and classifications of SSW that have been proposed [reviewed by Butler et al. (2015)], the current and most widely used definition of midwinter SSW was proposed as early as the 1970s by the World Meteorological Organization, and is described more explicitly in Charlton and Polvani (2007). The basic understanding regarding the dynamics of SSW is that enhanced planetary waves generate in the troposphere, propagate upwards into the stratosphere, break in the midlatitude stratosphere, and the wave forcing drives the polar temperature rise and slows the mean flow (Matsuno, 1971; Holton, 1976; Andrews et al., 1987).

The enhanced wave activities during SSWs potentially influence the wave-driven hemispheric overturning circulation, i.e., the Brewer–Dobson circulation (BDC) (Dobson et al., 1929; Brewer, 1949). This mechanism of wave-driven mean meridional circulation is referred to as the "downward control" principle (Haynes et al., 1991) or extratropical "wave pump" (Holton et al., 1995). In fact, the complete structure of the BDC is more complicated. There are two hemispheric branches of the BDC in the stratosphere: the deep branch, which penetrates high into the upper stratosphere; and the shallow branch, which overturns in the lower stratosphere (e.g. Plumb, 2002; Bönisch et al., 2011). The connection and disconnection between the two BDC branches have been intensively discussed. Some studies emphasize that the extratropical wave drives the entire tropical upwelling (both branches), with an equatorward propagation of about 10 days (Ueyama and Wallace, 2010; Ueyama et al., 2013). Other works suggest that the equatorial wave is important for driving upwelling at the tropical tropopause (e.g., Kerr-Munslow and Norton, 2006; Ryu and Lee, 2010). Several works suggest an alternative dynamical mechanism is responsible for the shallow branch circulation: combined extratropical and equatorial wave drag in the subtropics (Bönisch et al., 2011; Garny et al., 2011) that remotely influences the tropical upwelling through the zonal wind tendency from subseasonal to decadal timescales (Randel et al., 2008; Shepherd and McLandress, 2011; Abalos et al., 2014).

The SSW events that take place when the most pronounced enhancement of the planetary wave occurs on a sub-

* Corresponding author: Yuli ZHANG
Email: zhangyuli@mail.iap.ac.cn

seasonal timescale can be regarded as a natural experiment in which we can study the response of the BDC to the variable dynamics. Most previous works on the association between the BDC and SSWs have focused on the poleward and descending motion of the BDC at high latitudes from the perspective of dynamical anomalies (Labitzke and Kunze, 2009; Manney et al., 2009a; Liu et al., 2014), or from tracer transport (Manney et al., 2005, 2009b; Tao et al., 2015a) or ozone chemistry (Konopka et al., 2005; Kuttippurath and Nikulin, 2012). Several recent studies have noticed an increased tropical upwelling response to SSWs based on evidence from lower-stratospheric water vapor. Extratropical cooling and drying related to SSWs was found as a subseasonal variation of tropical lower-stratospheric water vapor by a 35-year simulation (Tao et al., 2015b), and the extra-drying effect was confirmed by in-situ water vapor measurements (Evan et al., 2015). Gómez-Escolar et al. (2014) proposed that SSWs induce strong tropical upwelling and extra cooling as a response to subtropical planetary wave breaking, which is modulated by the phases of the Quasi-Biennial Oscillation (QBO).

Since the tropical BDC response to SSWs has rarely been discussed in detail, and the effect is important for troposphere–stratosphere transport of climate-relevant species like H_2O and O_3, we focus in this study on the BDC response at different altitudes based on three remarkable SSWs that occurred in the 2000s. Then, we discuss the association of the deep and shallow branches of the BDC with the evolution of the wave forcing. Following this introduction, section 2 introduces the data and method used in the study. Section 3 provides an overview of the dynamical background, including the wind, temperature, polar vortex and planetary wave propagation during the three warming events. In section 4, we diagnose the strength of upwelling in the shallow and deep branches of the BDC during the SSWs. In section 5, the relationship between the BDC and wave forcing is discussed based on the Eliassen–Palm (EP) flux and its divergence in an isentropic coordinate. A discussion and a summary of the main findings of our study are provided in section 6.

2. Data and method

To estimate the zonal-mean mass transport by the BDC, the widely used definition of the mean meridional residual circulation in log-pressure coordinates is defined as

$$\overline{v}* = \overline{v} - \frac{1}{\rho_0}[(\rho_0\overline{v'\theta'})/\overline{\theta}_z]_z \,, \tag{1}$$

$$\overline{w}^* = \overline{w} + \frac{1}{a\cos\varphi}[(\cos\varphi\overline{v'\theta'})/\overline{\theta}_z]_\varphi \,, \tag{2}$$

where overbars indicate the zonal mean. The items ρ, a, v, w represent density, radius, meridional and vertical velocity (Andrews et al., 1987).

This study is performed in the isentropic coordinate, where φ and θ denote latitude and theta, respectively. The zonal mean residual circulation in the isentropic coordinate is defined as the isentropic mass density (σ) weighted mean meridional velocity ($\overline{v}^*$) and cross-isentropic velocity ($\overline{w}^*$):

$$\overline{v}^* = \overline{\sigma v} \,, \tag{3}$$

$$\overline{w}^* = \overline{\sigma\dot{\theta}} \,, \tag{4}$$

where the vertical velocity $\dot{\theta}$ can be estimated by the total diabatic heating rates ($\dot{\theta} = Q$). The advantage of using the isentropic coordinate is that no additional transformation is required, compared to the formalism in log-pressure coordinates in Andrews et al. (1987).

Typically, 70 hPa is used as the upper-limit pressure level [$\sim$ 500 K (20 km)$^{-1}$] of the shallow branch of the BDC (e.g. Rosenlof, 1995, Bönisch et al., 2011, Abalos et al., 2014). Here, we use the total positive $\overline{w}^*$ between 380 K and 500 K to quantify the upwelling of the shallow branch of the circulation, and the total positive $\overline{w}^*$ between 600 K and 1500 K to quantify the upwelling of the deep branch.

The wave forcing is diagnosed by the divergence of EP flux (e.g., Eliassen, 1951; Plumb and Bell, 1982). EP flux vectors represent the propagation direction of wave energy. More specifically, EP flux divergence characterizes the forcing from eddy (or wave) to the zonal mean flow. Here, we use the EP flux formula in an isentropic coordinate, referring to the TEM formalism by Andrews et al. (1987). The vertical and horizontal components of EP flux [$F = (F_\varphi, F_\theta)$] are given by

$$F_\varphi = -a\cos\varphi\overline{(\sigma v)'u'} \,, \tag{5}$$

$$F_\theta = (\overline{p'M'_\lambda}/g) - a\cos\varphi\overline{(\sigma Q)'u'} \,, \tag{6}$$

where M is the Montgomery streamfunction ($M = C_pT + gz$), p is pressure, and a is the Earth's radius. The Montgomery streamfunction is the streamfunction for the geostrophic flow, which is equal to $C_pT + gz$ on an isentropic surface, where z is the height of the isentropic surface.

The European Centre for Medium-Range Weather Forecasts interim reanalysis (ERA-Interim) dataset is used to study the dynamical background and to derive the eddy heat and momentum fluxes. The ERA-Interim data have a temporal resolution of 6 h and a horizontal resolution of $1.5^\circ \times 1.5^\circ$. Originally in a 37-layer pressure coordinate, the data are interpolated into a 60-layer hybrid coordinate between the pressure coordinate (below 300 hPa) and isentropic coordinate (above 300 hPa). The vertical cross-isentropic velocity ($\dot{\theta} = d\theta/dt$) is equal to the ERA-Interim forecast total diabatic heating rate (Q) (Ploeger et al., 2010). The rate of theta change following a parcel is equal to the total diabatic heating rate, which contains the effects of all-sky radiative heating, latent heat release, and diffusive heating.

The methodology to identify the onset of the SSWs is based on Charlton and Polvani (2007). The main criterion of this method to identify SSW events is the reversal of the zonal mean zonal wind at 10 hPa and 60°N during November–March [see Charlton and Polvani (2007) for more details]. In addition, the magnitude of an SSW event is measured by the

Table 1. Key information regarding the three SSW events selected in this study. The dominant wavenumber is determined by the amplitude of wave components averaged over 40°–70°N at 400 K through Fourier decomposition. The vortex geometry during the SSWs is determined by checking the daily potential vorticity map in the Northern Hemisphere. The QBO phase for each SSW is defined as the 30-day smoothed equatorial mean wind at $\theta = 500$ K (~ 50 hPa), calculated for each SSW central date.

Year	Central date	Magnitude ΔT_{10} (K)	Planetary wavenumber	Polar vortex geometry	QBO phase
2003/04	5 Jan 2004	12.5	wavenumber-1	Displaced	Easterly
2005/06	21 Jan 2006	7.7	wavenumber-1	Displaced	Easterly
2008/09	24 Jan 2009	14.4	wavenumber-2	Split	Westerly

mean temperature anomaly over the polar cap (60°–90°N) at 10 hPa (ΔT_{10}, shown in Table 1), and the polar vortex edge is identified by the maximum potential vorticity meridional gradient combined with the maximum westerlies [further details in Nash et al. (1996)].

The QBO is a major impact factor of tropical upwelling and tropical temperature in the stratosphere, inducing temperature variations of ±4 K and ±0.5 K in the lower stratosphere and around the tropopause, respectively (Baldwin et al., 2001; Xie et al., 2014). Although El Niño–Southern Oscillation (ENSO) is an important tropospheric factor (Xie et al., 2012, 2014), Konopka et al. (2016) suggested that, whilst there is a three-dimensional impact of ENSO on tropical upwelling, it is not as pronounced as that of the QBO in a zonal-mean sense. Thus, the QBO phase during the SSW period, and not the ENSO phase, is considered in this study. The QBO phase for each SSW event is defined as the 30-day smoothed equatorial mean wind at $\theta = 500$ K (~ 50 hPa), calculated for each SSW central date.

3. Dynamical background

The 20-year de-seasonalized (referred to as the climatology from 1979 to 2013) records of averaged polar cap temperature and mean zonal wind around the North Pole (55°–65°N) are shown in Fig. 1. A ±7-day smoothing is applied to both the temperature and wind data to remove the short-term variations, e.g., synoptic perturbation. We can see that SSW events are the most pronounced subseasonal variation during boreal winter. There are nine major SSWs during the 20 years. The black arrows mark the central dates of all the major SSWs, according to Charlton and Polvani (2007). Note that in this study we follow the recommendation of Butler et al. (2015) to use the mean zonal wind from 55°–65°N, instead of the zonal wind at a specific latitude such as 60°N.

Among all the major SSWs, three events during the boreal winters of 2003/04, 2005/06 and 2008/09 are the most remarkable. Table 1 provides the essential information about these three remarkable SSWs, including their central dates, magnitudes of temperature rise, dominant planetary wavenumbers, polar vortex geometries, and QBO phases in the tropics. Firstly, the three SSWs experience the strongest temperature and wind variation, which can be quantified by the polar cap temperature increase listed in Table 1 as ΔT_{10}. Secondly, the perturbation of temperature and wind descend more deeply to the lower stratosphere and the upper troposphere during the three SSWs than in the other SSWs. Thirdly, all three SSWs are followed by strong polar vortex recovery, shown as the strong cooling and westerly anomalies after their occurrence. This polar warm and cold oscillation in boreal winter refers to the polar-night jet oscillation (e.g., Kuroda and Kodera, 2001; Hitchcock and Shepherd, 2013). This is the result of radiative relaxation, diabatic cooling in the polar region, as well as the suppression of planetary wave propagation into the high latitudes due to the formation of easterlies.

The SSWs in 2003/04 and 2005/06 both correspond to an increasing wavenumber-1, whereas the warming event in 2008/09 is driven by a rapid increase in wavenumber-2 (Manney et al., 2005, 2008, 2009a, 2009b). The geometry of the polar vortex during the SSWs is closely associated with the dominant planetary wave: wavenumber-1 and wavenumber-2 usually lead to vortex-displacement and vortex-split events, respectively. Moreover, the SSWs in 2003/04 and 2005/06 both occur during an easterly QBO phase in the tropics, whereas the SSW in 2008/09 occurs during a westerly QBO phase. Therefore, the three cases include different wavenumber and QBO situations, and are thus representative of various dynamical backgrounds.

4. Response of the BDC

Aside from the intense change in wind and temperature during SSWs, a dramatic enhancement in vertical mass transport is also noticeable. Figure 2 shows the anomalies of the diabatic heating rate ($\dot{\theta}$) in the polar region (left-hand column) and tropical region (right-hand column). The anomalies of $\dot{\theta}$ over the North Pole and tropics illustrate the evolution of the polar downwelling and tropical upwelling of the BDC, respectively. We can see that enhanced downwelling (negative anomalies) occurs in the upper stratosphere and propagates downwards gradually to 500 K after 10–15 days.

The negative anomalies at upper levels (e.g., 1000 K) are only sustained for less than one month (only 10 days in the 2009 case), whereas in the lower stratosphere the intensified descent lasts longer than two months. The time scales are consistent with radiative relaxation time scales: 10 days in the upper stratosphere and around 100 days in the lower stratosphere (Mlynczak et al., 1999).

Besides, the left-hand column shows the acceleration of polar descent (negative anomalies) is always followed by strong deceleration of polar descent (positive anomalies) in

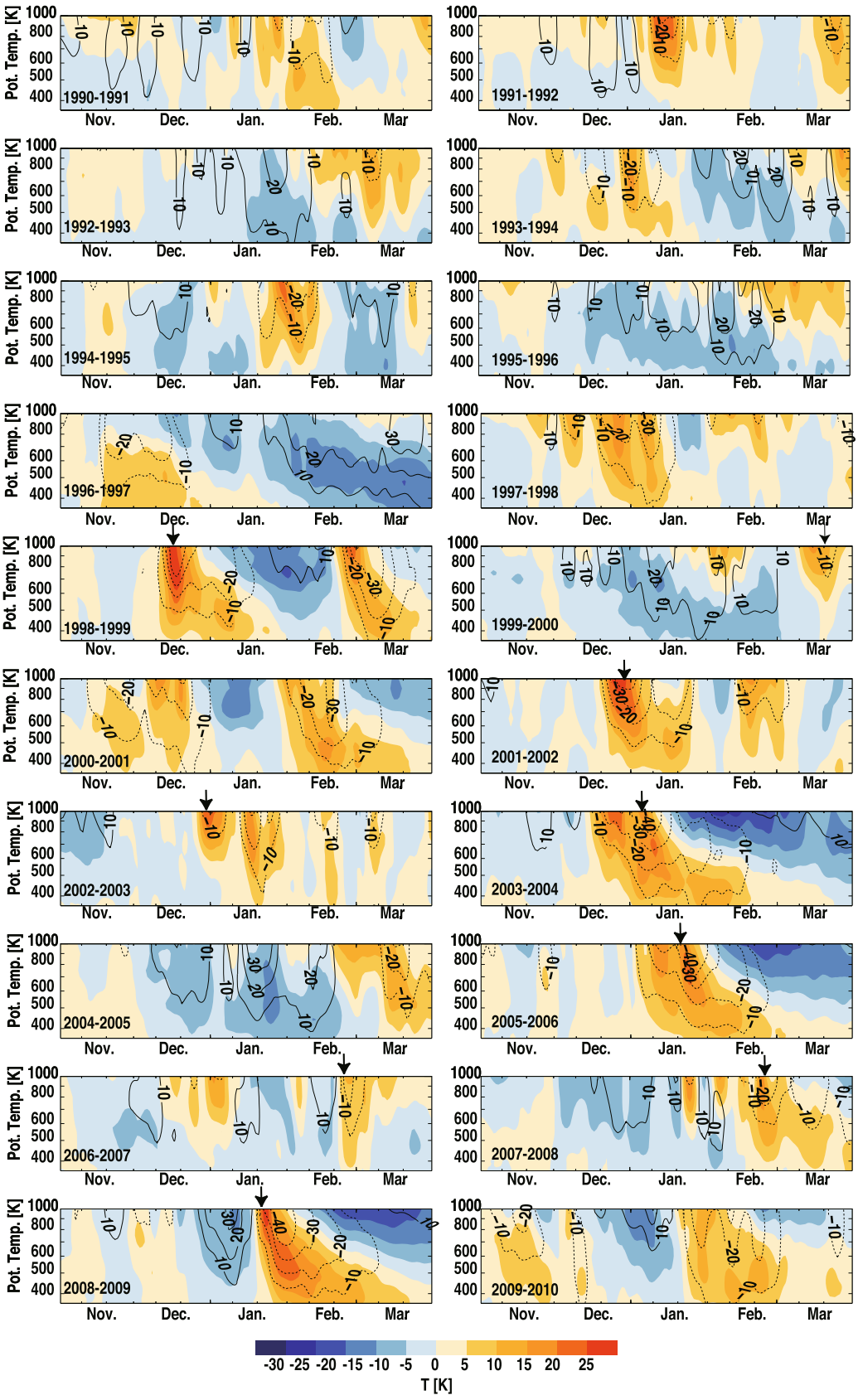

Fig. 1. De-seasonalized temperature (color shading) at the North Pole (60°–90°N) and zonal mean wind between 55°N and 65°N (positive: solid contours; negative: dashed contours; values larger than 10 m s^{-1} shown) during boreal winter (November–March) from 1990 to 2009. A ±7-day running mean is applied to both the temperature and zonal wind. Black arrows point to the central dates of the SSWs (Charlton and Polvani, 2007).

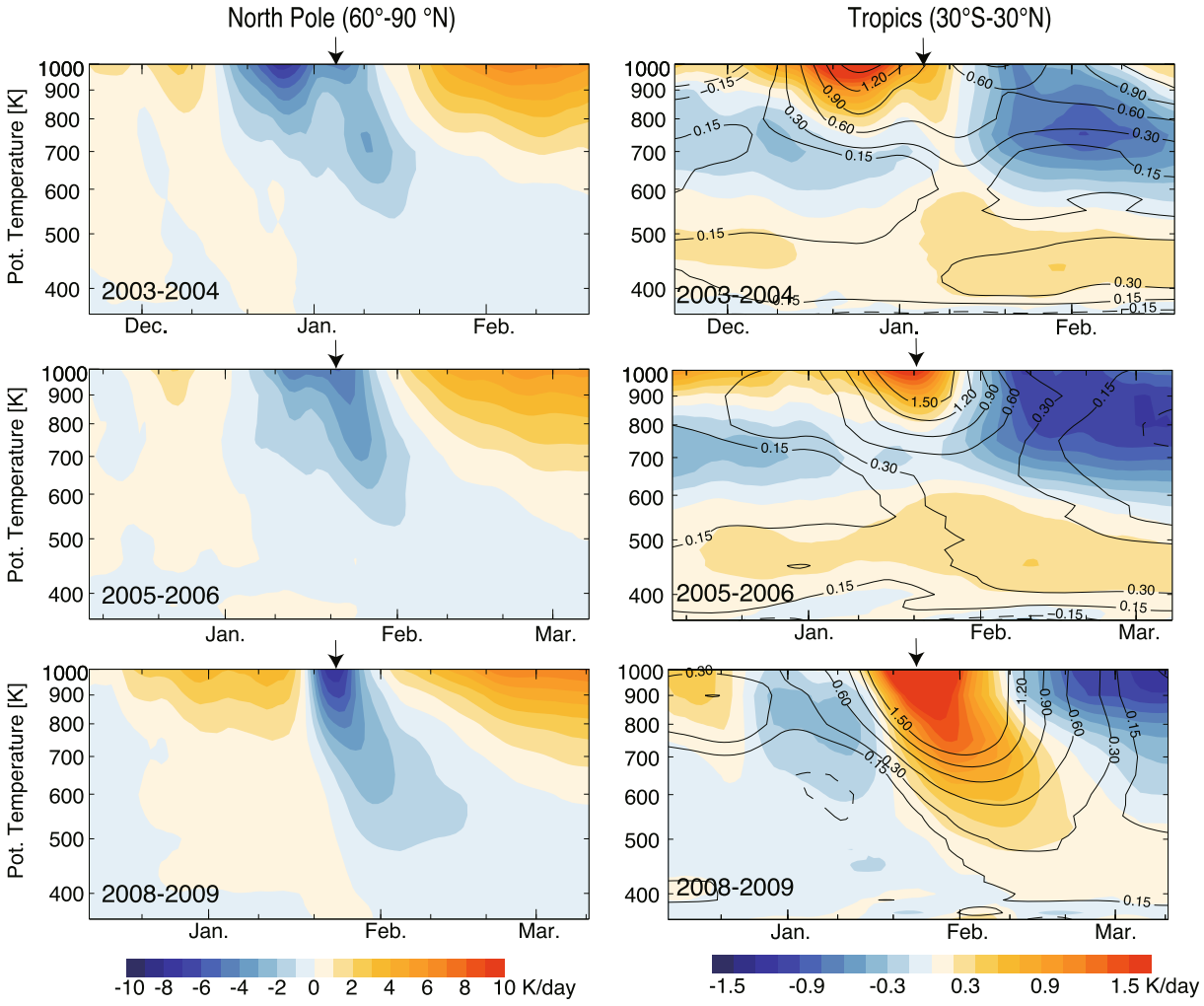

Fig. 2. De-seasonalized cross-isentropic velocity ($\dot{\theta}$) averaged over the North Pole (60°–90°N; left column) and over the tropics (30°S–30°N; right column), shown respectively for the 2003/04 (top), 2005/06 (middle) and 2008/09 (bottom) winters. Contours in the right-hand panels show the anomalies referring to the corresponding climatology in the same QBO phase. Black arrows indicate the central dates of the SSWs (Charlton and Polvani, 2007).

the upper stratosphere. This deceleration of polar descent corresponds to a strong polar vortex recovery due to radiative cooling. It is also worth mentioning that the negative anomaly during the 2008/09 SSW has the most intense amplitude (velocity decreasing to -10 K d^{-1} at 1000 K), the fastest recovery at 1000 K (only 10 days for 2008/09; one month for the other two events), and the quickest arrival in the lower stratosphere (< 10 days for 2008/09; 15 days for the other two).

The impact of the SSWs is not only confined to the polar region, but also extends to the tropics. Along with the intensified polar descent, tropical upwelling also enhances, which can be seen as the positive anomalies in the right-hand column of Fig. 2. Note that two anomalies are shown in the right-hand column: the anomalies referring to the climatology (de-seasonalized anomalies; color shading); and the anomalies referring to the easterly QBO (eQBO)/ westerly QBO (wQBO) climatology (de-seasonalized and de-QBO anomalies; black contours). Both quantities also indicate that the response of tropical upwelling to the SSWs starts simultaneously with the polar downwelling beginning to accelerate in the upper stratosphere. Disconnection between the deep and shallow BDC can be observed in the 2003/04 and 2005/06 cases: the descent of upwelling positive anomalies from the upper stratosphere pauses at around 500 K, but continues with a lag time in the lower stratosphere. The disconnection between the two branches is consistent with a previous work (Plumb, 2002; Bönisch et al., 2011), but also suggests a potential connection with a lagged effect due to latitudinal propagation (Ueyama and Wallace, 2010; Ueyama et al., 2013).

The difference in the tropical and polar regional mean is not significant. Figure 3 shows the evolution of the two (de-seasonalized and de-QBO) anomalies along the latitudes on the 1000 K (~ 10 hPa) and on the 450 K isentropic surface (~ 80 hPa). The enhancement of upwelling on the 1000 K surface reaches a maximum around the central dates (10 days earlier than the central date for the 2003/04 case) and lasts for 10–20 days. The differences in the two (de-seasonalized and

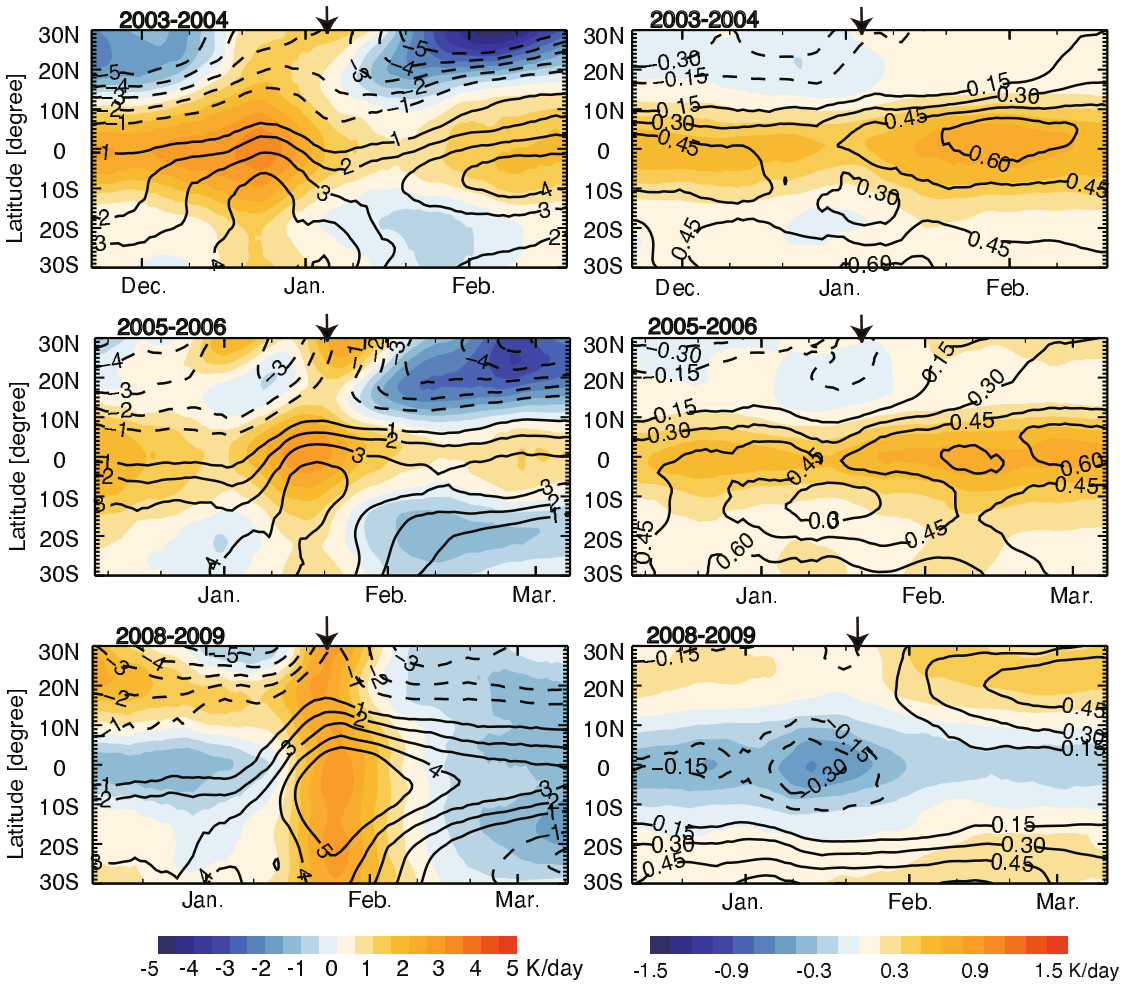

Fig. 3. De-seasonalized zonal mean cross-isentropic velocity ($\dot{\theta}$) on the 400 K isentropic surface, shown as color shading, for the 2003/04 (top), 2005/06 (middle) and 2008/09 (bottom) winters. Contours show the anomalies referring to the corresponding climatology in the same QBO phase. Black arrows indicate the central dates of the SSWs (Charlton and Polvani, 2007).

de-QBO) upwelling anomalies on the 1000 K surface (left-hand panels) are noticeable: although the de-seasonalized upwelling enhances roughly hemisphere-symmetrically after the SSW and is centered at equator, the positive anomalies referring to the QBO climatology shift more to the Southern Hemisphere. The asymmetry of the de-QBO anomalies is not significant for the upwelling in the lower stratosphere (right-hand panels). Enhanced upwelling of the shallow BDC in the Northern Hemisphere is also found following the three SSWs, but the peak of the positive anomalies happens 20–30 days after the SSWs, when the upwelling for the deep branch starts to decrease.

Figure 4 sums up the BDC response to the SSWs by quantifying the strength of the deep branch upwelling anomalies (black lines) and shallow branch upwelling anomalies (gray lines). Here, we use the total positive (upward) vertical component of residual circulation $\overline{w}^*$ over the regions 30°S–30°N between 600 K and 1500 K and 30°S–30°N between 380 K and 500 K, representing the deep and shallow branches of the BDC upwelling, respectively. These quantities are proportional to the upward mass fluxes crossing the isentropic surface [see Eq. (4)]. Note that the corresponding QBO climatology is used for calculating the relative differences. Thus, the values in Fig. 4 stand for the relative anomalies from the QBO climatology (units: %).

We find that the deep branch upwelling quickly increases with large variability before the SSWs commence, whereas it decreases sharply 10 days afterwards. The increase in amplitude of the upwelling of the deep BDC reaches 20% for the 2003/04 and 2005/06 cases, and 30% for the 2008/09 case. The shallow branch upwelling remains almost constant, with some variations before the start of the SSWs, before slowly accelerating and reaching a peak within a month. The enhancement of the shallow BDC upwelling after the SSW cases reaches a maximum of 40% in the 2003/04 and 2005/06 cases, and 20% in the 2008/09 case. The contribution from the two hemispheres varies from case to case. Compared with the shallow branch upwelling in the Northern Hemisphere, the variation of upwelling in the Southern Hemisphere is not significant (Fig. 3).

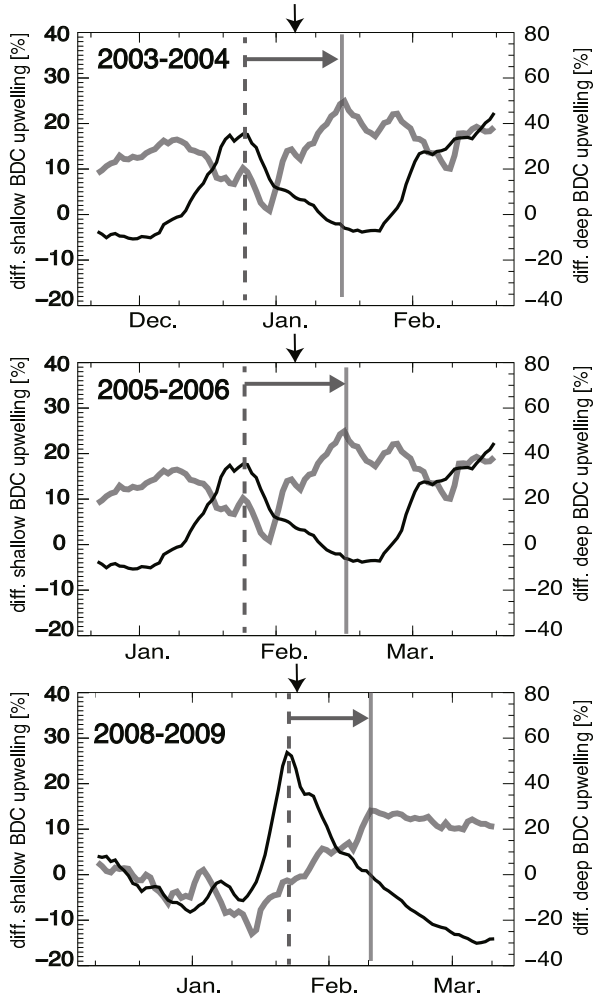

Fig. 4. Variation in tropical upwelling relative differences from the corresponding QBO phase climatology ($\dot{\bar{w}}^*$), shown for the total shallow BDC (gray lines) and deep branch of the BDC (black lines). The total positive $\dot{\bar{w}}^*$ over 30°S–30°N between 600 K and 1500 K denotes the deep branch upwelling. The total positive $\dot{\bar{w}}^*$ over 30°S–30°N between 380 K and 500 K represents the shallow branch upwelling. Arrows mark the central dates of the SSWs. Dashed straight lines mark the peak of the black lines (strongest upwelling for deep BDC), and solid straight lines mark the peak of the grey lines (strongest upwelling for shallow BDC).

5. Wave forcing

Following discussion of the lagged evolution from the deep to shallow branch upwelling in the previous section, we next study the associated wave activities driving the circulation. Figure 5 shows the evolution of Northern Hemisphere EP flux divergence at selected locations, shown as "A" and "B" in Fig. 6, during the ±45 days around the central date. Note that a five-day running mean has been applied to the quantities in Fig. 5. The black line represents the wave forcing in the mid-to-upper stratosphere. We can see that the black lines all reach a minimum (largest EP flux convergence) around the central date of the SSW, and all gradually increase afterwards. The gray lines clearly have a similar phase to the black lines shown in the deep BDC variation in Fig. 5. The correlation coefficients between the two quantities are about −0.6 in all three cases. The negative correlation between the evolution of equatorward upwelling and EP flux divergence indicates in-phase wave forcing (negative EP flux divergence) of the upwelling according to the "downward control" principle (Haynes et al., 1991).

Similar to the lagged response from the deep to shallow BDC, we see a 20–40-day lagged evolution of the subtropical lower stratosphere (grey lines) to the pronounced subseasonal variation of EP flux divergence at high latitudes in the mid-to-upper stratosphere in all three cases. Although a small-scale wave, e.g., a synoptic wave or gravity wave, could have contributed to the wave drag of tropical upwelling, the subtropical planetary wave forcing (gray lines) in the lower stratosphere revealed by the ERA-Interim data shows a close association with the shallow branch BDC. The EP flux divergence gradually decreases before the central dates, and continuously decreases afterwards. The maximum wave forcing (minimum EP flux divergence) is found around 20–40 days

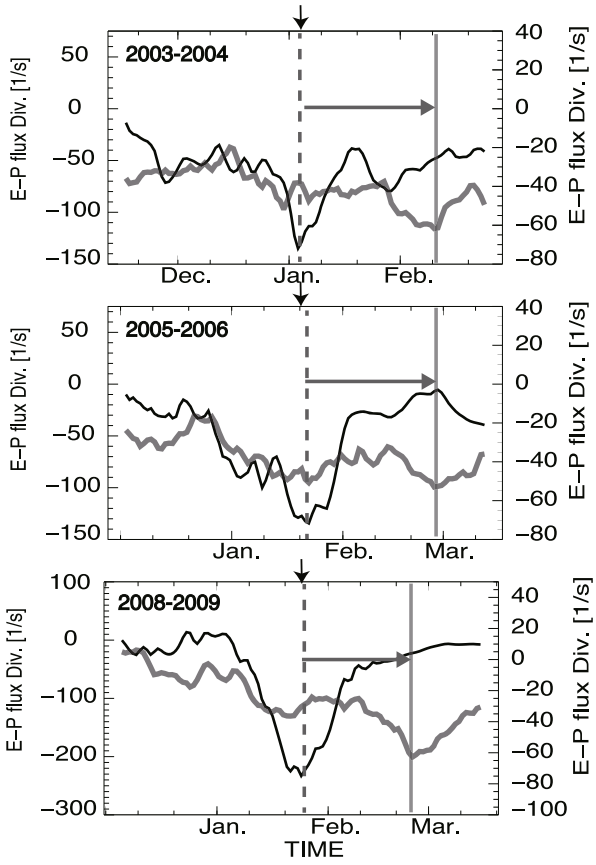

Fig. 5. Evolution of EP flux divergence during the three SSW events. Black lines show the EP flux divergence at (50°N, θ = 800 K; marked "A" in Fig. 6). Gray lines show the EP flux divergence at (15°N, θ = 450 K; marked "B" in Fig. 6). The central date of each SSW is marked by an arrow. Dashed lines mark the minimum of the black lines (strongest wave forcing), and the solid lines mark the minimum of the gray lines (strongest wave forcing). A five-day running mean is applied to the quantities.

after the central dates. The gray lines in Fig. 5 again illustrate a close evolution with the upwelling of the shallow BDC (gray lines) in Fig. 4. The correlation coefficients between the two quantities are about −0.5 for the selected cases, which suggests a relationship between subtropical wave forcing in the Northern Hemisphere and shallow tropical upwelling.

To follow this method and to explore the relationship between the wave forcing and the two branches of the BDC and its relationship with zonal wind, we further apply correlation analysis to the variation in EP flux divergence with that of the shallow and deep BDC upwelling during ±45 days around the central dates in Fig. 6. We analyze the correlation in the variation of EP flux divergence with the variation in the shallow and deep branch upwelling shown in Fig. 5 (the area used for calculating the BDC upwelling is indicated by the red square). Note that, before the correlation analysis, a five-day running mean is applied to the EP flux divergence shown in Fig. 6. The regions within which the correlation of

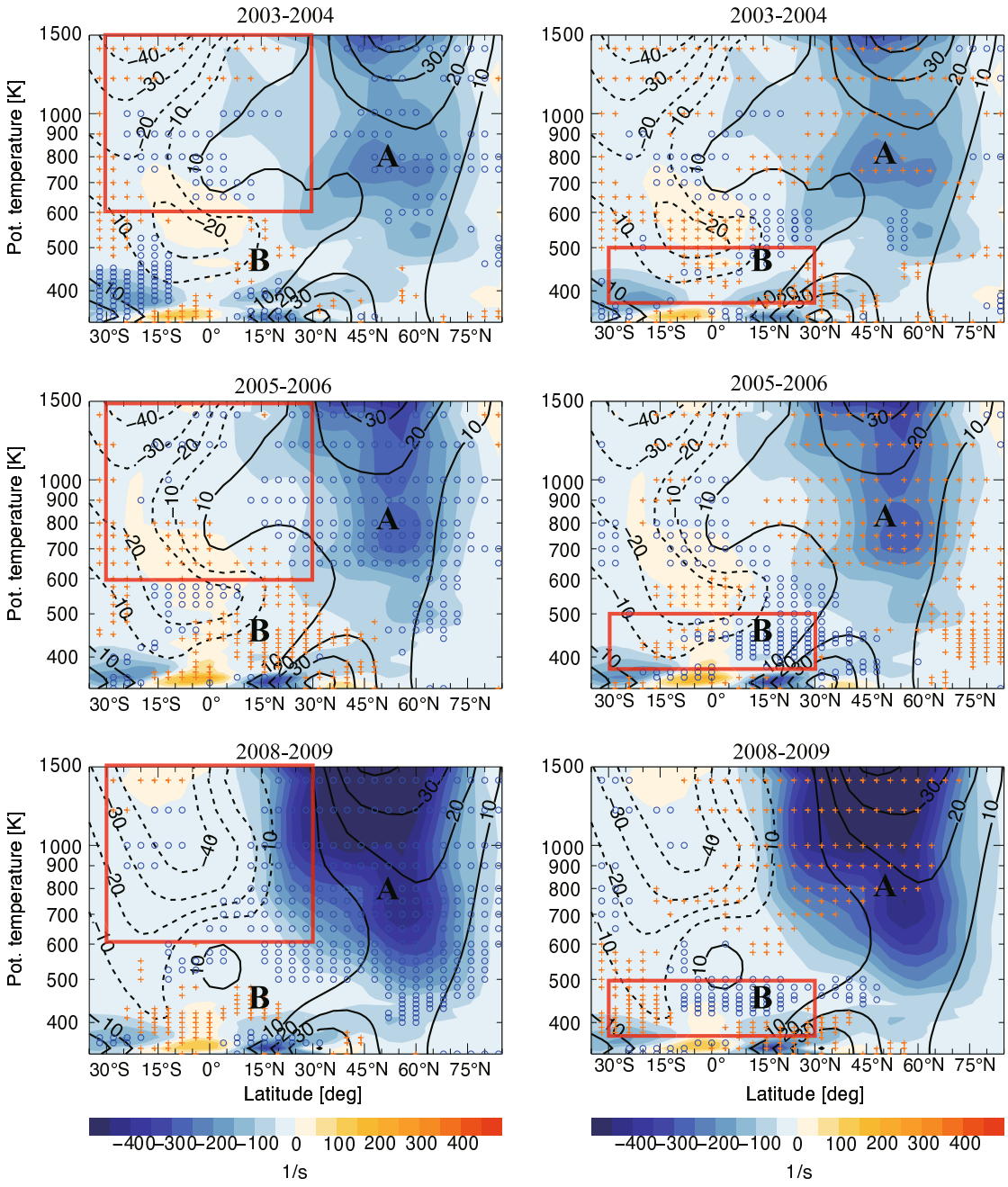

Fig. 6. Latitude–height projections of EP flux divergence (color shading) averaged over ±10 days around the central dates. Solid and dashed contours show the westerly and easterly zonal mean wind averaged over ±45 days around the central dates. Regions where the correlation of the EP flux divergence with the variation of upwelling over the red-square region (left-hand column: 30°S–30°N, 600–1500 K; right-hand column: 30°S–30°N, 380–500 K) pass the 95% significance test are marked by yellow crosses (positive correlation) and blue circles (negative correlation).

EP flux divergence with the tropical upwelling is statistically significant (*t*-test; 0.95 significance level) are overlaid with orange crosses (positive correlation) or blue dots (negative correlation). Recall here that negative correlation (blue dots) suggests the corresponding wave forcing could be the wave drag to the correlated upwelling, according to the "downward control" principle, as shown in the relationship in Fig. 4 and Fig. 5. Positive correlation (orange crosses) indicates a lag time between the subseasonal variation of wave forcing and the correlated upwelling.

All three cases suggest that the deep branch of the BDC upwelling is mainly a response to the high-latitude EP flux convergence or extratropical planetary wave drag in the mid-to-upper stratosphere (blue dots in the left-hand panels of Fig. 6). An example is the EP flux divergence variation of location "A" shown in Fig. 6 (black lines). On the other hand, the wave drag correlated with the upwelling of the shallow BDC shows an almost opposite correlation with wave forcing: its acceleration is positively correlated with the high-latitude EP flux divergence in the mid-to-upper stratosphere (near "A") and negatively correlated to the EP flux divergence in the subtropics between 400 K and 500 K (near "B"). The positive correlation of extratropical wave drag indicates the lagged effect from the wave drag for the deep BDC to that for the shallow BDC. A significantly negatively correlated subtropical wave drag can be a remote forcing for enhanced shallow upwelling in the tropics (Garcia, 1987).

The propagation and breaking of the wave interacts with the background zonal wind shown as contours in Fig. 6 (Dickinson, 1968). Before the SSWs, strong westerlies in the high latitudes favor the upward propagation of planetary waves more poleward, and breaks at high latitudes. After the SSWs, when the extratropical westerlies have been largely weakened or reversed to easterlies, further wave propagation into the stratosphere either breaks at the bottom of the extratropical easterlies, or breaks at the tropics close to the zero-wind line (Gómez-Escolar et al., 2014). As seen in the right-hand panels of Fig. 6, the significant correlation of subtropical wave drag is mainly located where the zonal wind is close to zero. As proposed by Gómez-Escolar et al. (2014), the QBO phase is important for the location of the zero-wind line, and thus important to the breaking of waves driving the lower-stratospheric upwelling.

6. Conclusion and discussion

The three remarkable mid-winter SSW events studied here all show strong subseasonal temperature, wind and cross-isentropic velocity variability from the middle of winter to spring, throughout the Northern Hemispheric stratosphere. The response of the tropical upwelling of the shallow branch of the BDC must be discussed separately to the deep branch because they show a different tendency and a lagged enhancement after the SSWs. Our results suggest that the strength of the deep branch of the BDC reaches a peak around the central date of the SSW, and rapidly decreases afterwards. On the other hand, the shallow branch of the BDC gradually accelerates after the SSW central date, remaining for more than one month in all three cases.

The result suggests a disconnection between the deep and shallow branches of the BDC, which show different variation after the SSW, but also a connection between the two branches in the form of a lagged enhancement from the deep branch to the shallow branch. This case study result is consistent with results from composite analysis by Gómez-Escolar et al. (2014), in that the tropical BDC acceleration is a response to SSW events. Moreover, the modulation by the QBO of the shallow BDC upwelling is also confirmed in our present study: the 2008/09 (wQBO) case shows a weaker increase of upwelling in the lower stratosphere compared with the other two (eQBO) cases.

We also test the result of increased upwelling as a response to SSWs in more cases. The evolutions of mean upwelling of the deep and shallow BDC during years with and without SSWs during each QBO phase are compared. For the detailed method of case sampling and the identification of central dates (Charlton and Polvani, 2007), refer to Tao et al. (2015b). The result, shown in Fig. 7, includes all years

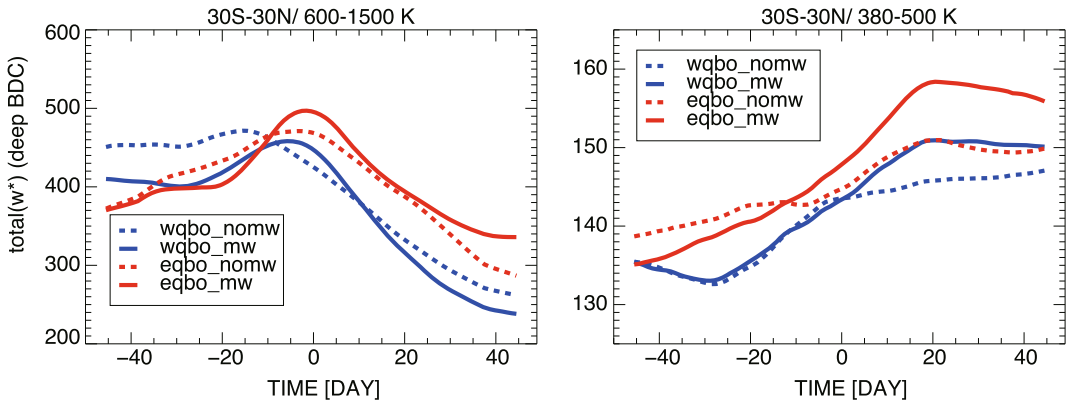

Fig. 7. Mean evolution of total positive tropical upwelling ($\bar{\dot{w}}^*$) of the deep branch (30°S–30°N, 600–1500 K) and shallow branch (30°S–30°N, 380–500 K) for all SSWs in eQBO (red solid line) and wQBO years (blue solid line), and winters without SSW in eQBO (red dashed line) and wQBO (blue dashed line) phases. Zero days for winter with SSWs are the central dates of each SSW and are the mean central dates for SSWs in each QBO phase for the years without SSWs.

with SSWs (1979–2013: eight wQBO cases and eight eQBO cases) and the years without SSWs (five eQBO cases and seven wQBO cases) in each QBO phase. Note here that the subseasonal variation is largely smoothed out by composition. Nevertheless, the composite still shows BDC enhancement due to SSWs for both branches, with a 20–30-day delay in both QBO phases, which supports the conclusion based on the case study.

Further analysis of wave forcing shows the deep and shallow BDC responding to the extratropical planetary wave forcing and the subtropical planetary wave drag, respectively. The lagged and remote connection between the extratropical and subtropical wave drag can be explained by the variation in the zonal wind background, consistent with previous works (e.g., Dickinson, 1968; Garcia, 1987).

The variations in dynamics in the tropical lower stratosphere influence the transport from the troposphere to the stratosphere. This work supports and completes the theory of extra drying at a cooler tropopause associated with SSW events, as suggested by the simulation in Tao et al. (2015b) and from in-situ observations in Evan et al. (2015), from the dynamical perspective. Furthermore, the complex interaction between the variation in temperature, chemical reaction rates, and radiation effect, needs further investigation.

REFERENCES

Abalos, M., W. J. Randel, and E. Serrano, 2014: Dynamical forcing of subseasonal variability in the tropical Brewer-Dobson circulation. *J. Atmos. Sci.*, **71**, 3439–3453, doi: 10.1175/JAS-D-13-0366.1.

Andrews, D. G., J. R. Holton, and C. B. Leovy, 1987: *Middle Atmosphere Dynamics*. Academic Press, Orlando, USA, 489 pp.

Baldwin, M. P., and Coauthors, 2001: The quasi-biennial oscillation. *Rev. Geophys.*, **39**, 179–229, doi: 10.1029/1999RG000073.

Bönisch, H., A. Engel, T. Birner, P. Hoor, D. W. Tarasick, and E. A. Ray, 2011: On the structural changes in the Brewer-Dobson circulation after 2000. *Atmospheric Chemistry and Physics*, **11**, 3937–3948, doi: 10.5194/acp-11-3937-2011.

Brewer, A. W., 1949: Evidence for a world circulation provided by the measurements of helium and water vapour distribution in the stratosphere. *Quart. J. Roy. Meteor. Soc.*, **75**, 351–363, doi: 10.1002/qj.49707532603.

Butler, A. H., D. J. Seidel, S. C. Hardiman, N. Butchart, T. Birner, and A. Match, 2015: Defining sudden stratospheric warmings. *Bull. Amer. Meteor. Soc.*, **96**, 1913–1928, doi: 10.1175/BAMS-D-13-00173.1.

Charlton, A. J., and L. M. Polvani, 2007: A new look at stratospheric sudden warmings. Part I: Climatology and modeling benchmarks. *J. Climate*, **20**, 449–469, doi: 10.1175/JCLI3996.1.

Dickinson, R. E., 1968: Planetary Rossby waves propagating vertically through weak westerly wind wave guides. *J. Atmos. Sci.*, **25**, 984–1002, doi: 10.1175/1520-0469(1968)025<0984:PRWPVT>2.0.CO;2.

Dobson, G. M. B., D. N. Harrison, and J. Lawrence, 1929: Measurements of the amount of ozone in the Earth's atmosphere and its relation to other geophysical conditions. Part III. *Proc. Roy. Soc. London*, **122**, 456–486, doi: 10.1098/rspa.1929.0034.

Eliassen, A., 1951: Slow thermally or frictionally controlled meridional circulation in a circular vortex. *Astrophysica Norvegica*, **5**, 19.

Evan, S., K. H. Rosenlof, T. Thornberry, A. Rollins, and S. Khaykin, 2015: TTL cooling and drying during the January 2013 stratospheric sudden warming. *Quart. J. Roy. Meteor. Soc.*, **141**, 3030–3039, doi: 10.1002/qj.2587.

Garcia, R. R., 1987: On the mean meridional circulation of the middle atmosphere. *J. Atmos. Sci.*, **44**, 3599–3609, doi: 10.1175/1520-0469(1987)044<3599:OTMMCO>2.0.CO;2.

Garny, H., M. Dameris, W. Randel, G. E., Bodeker, and R. Deckert, 2011: Dynamically forced increase of tropical upwelling in the lower stratosphere. *J. Atmos. Sci.*, **68**, 1214–1233, doi: 10.1175/2011JAS3701.1.

Gómez-Escolar, M., N. Calvo, D. Barriopedro, and S. Fueglistaler, 2014: Tropical response to stratospheric sudden warmings and its modulation by the QBO. *J. Geophys. Res.*, **119**, 7382–7395, doi: 10.1002/2013JD020560.

Haynes, P. H., M. E. McIntyre, T. G. Shepherd, C. J. Marks, and K. P. Shine, 1991: On the "downward control" of extratropical diabatic circulations by eddy-induced mean zonal forces. *J. Atmos. Sci.*, **48**, 651–678, doi: 10.1175/1520-0469(1991)048<0651:OTCOED>2.0.CO;2.

Hitchcock, P., and T. G. Shepherd, 2013: Zonal-mean dynamics of extended recoveries from stratospheric sudden warmings. *J. Atmos. Sci.*, **70**, 688–707, doi: 10.1175/JAS-D-12-0111.1.

Holton, J. R., 1976: A semi-spectral numerical model for wave-mean flow interactions in the stratosphere: Application to sudden stratospheric warmings. *J. Atmos. Sci.*, **33**, 1639–1649, doi: 10.1175/1520-0469(1976)033<1639:ASSNMF>2.0.CO;2.

Holton, J. R., P. H. Haynes, M. E. McIntyre, A. R. Douglass, R. B. Rood, and L. Pfister, 1995: Stratosphere-troposphere exchange. *Rev. Geophys.*, **33**, 403–439, doi: 10.1029/95RG02097.

Kerr-Munslow, A. M., and W. A. Norton, 2006: Tropical wave driving of the annual cycle in tropical tropopause temperatures. Part I: ECMWF analyses. *J. Atmos. Sci.*, **63**, 1410–1419, doi: 10.1175/JAS3697.1.

Konopka, P., J.-U. Grooß, K. W. Hoppel, H.-M. Steinhorst, and R. Müller, 2005: Mixing and chemical ozone loss during and after the Antarctic polar vortex major warming in September 2002. *J. Atmos. Sci.*, **62**, 848–859, doi: 10.1175/JAS-3329.1.

Konopka, P., F. Ploeger, M. C. Tao, and M. Riese, 2016: Zonally resolved impact of ENSO on the stratospheric circulation and water vapor entry values. *J. Geophys. Res.*, **121**, 11 486–11 501, doi: 10.1002/2015JD024698.

Kuroda, Y., and K. Kodera, 2001: Variability of the polar night jet in the northern and southern hemispheres. *J. Geophys. Res.*, **106**, 20 703–20 713, doi: 10.1029/2001JD900226.

Kuttippurath, J., and G. Nikulin, 2012: A comparative study of the major sudden stratospheric warmings in the arctic winters 2003/2004-2009/2010. *Atmospheric Chemistry and Physics*, **12**, 8115–8129, doi: 10.5194/acp-12-8115-2012.

Labitzke, K., and M. Kunze, 2009: On the remarkable arctic winter in 2008/2009. *J. Geophys. Res.*, **114**, D00I02, doi: 10.1029/2009JD012273.

Liu, C. X., B. J. Tian, K.-F. Li, G. L. Manney, N. J. Livesey, Y. L. Yung, and D. E. Waliser, 2014: Northern hemisphere mid-winter vortex-displacement and vortex-split stratospheric

sudden warmings: Influence of the madden-Julian oscillation and quasi-biennial oscillation. *J. Geophys. Res.*, **119**, 12 599–12 620, doi: 10.1002/2014JD021876.

Manney, G. L., M. L. Santee, N. J. Livesey, L. Froidevaux, W. G. Read, H. C. Pumphrey, J. W. Waters, and S. Pawson, 2005: EOS Microwave Limb Sounder observations of the Antarctic polar vortex breakup in 2004. *Geophys. Res. Lett.*, **32**, L12811, doi: 10.1029/2005GL022823.

Manney, G. L., and Coauthors, 2008: The evolution of the stratopause during the 2006 major warming: Satellite data andassimilated meteorological analyses. *J. Geophys. Res.*, **113**, D11115, doi: 10.1029/2007JD009097.

Manney, G. L., and Coauthors, 2009a: Satellite observations and modeling of transport in the upper troposphere through the lower mesosphere during the 2006 major stratospheric sudden warming. *Atmospheric Chemistry and Physics*, **9**, 4775–4795, doi: 10.5194/acp-9-4775-2009.

Manney, G. L., and Coauthors, 2009b: Aura microwave limb sounder observations of dynamics and transport during the record-breaking 2009 arctic stratospheric major warming. *Geophys. Res. Lett.*, **36**, L12815, doi: 10.1029/2009GL038586.

Matsuno, T., 1971: A dynamical model of the stratospheric sudden warming. *J. Atmos. Sci.*, **28**, 1479–1494, doi: 10.1175/1520-0469(1971)028<1479:ADMOTS>2.0.CO;2.

Mlynczak, M. G., C. J. Mertens, R. R. Garcia, and R. W. Portmann, 1999: A detailed evaluation of the stratospheric heat budget: 2. Global radiation balance and diabatic circulations. *J. Geophys. Res.*, **104**, 6039–6066, doi: 10.1029/1998JD200099.

Nash, E. R., P. A. Newman, J. E. Rosenfield, and M. R. Schoeberl, 1996: An objective determination of the polar vortex using Ertel's potential vorticity. *J. Geophys. Res.*, **101**, 9471–9478, doi: 10.1029/96JD00066.

Ploeger, F., P. Konopka, G. Günther, J.-U. Grooß, and R. Müller, 2010: Impact of the vertical velocity scheme on modeling transport in the tropical tropopause layer. *J. Geophys. Res.*, **115**, D03301, doi: 10.1029/2009JD012023.

Plumb, R. A., 2002: Stratospheric transport. *J. Meteor. Soc. Japan*, **80**, 793–809, doi: 10.2151/jmsj.80.793.

Plumb, R. A., and R. C. Bell, 1982: A model of the quasi-biennial oscillation on an equatorial beta-plane. *Quart. J. Roy. Meteor. Soc.*, **108**, 335–352, doi: 10.1002/qj.49710845604.

Randel, W. J., R. Garcia, and F. Wu, 2008: Dynamical balances and tropical stratospheric upwelling. *J. Atmos. Sci.*, **65**, 3584–3595, doi: 10.1175/2008JAS2756.1.

Rosenlof, K. H., 1995: Seasonal cycle of the residual mean meridional circulation in the stratosphere. *J. Geophys. Res.*, **100**, 5173–5191, doi: 10.1029/94JD03122.

Ryu, J.-H., and S. Lee, 2010: Effect of tropical waves on the tropical tropopause transition layer upwelling. *J. Atmos. Sci.*, **67**, 3130–3148, doi: 10.1175/2010JAS3434.1.

Shepherd, T. G., and C. McLandress, 2011: A robust mechanism for strengthening of the Brewer-Dobson circulation in response to climate change: Critical-layer control of subtropical wave breaking. *J. Atmos. Sci.*, **68**, 784–797, doi: 10.1175/2010JAS3608.1.

Tao, M., P. Konopka, F. Ploeger, J.-U. Grooß, R. Müller, C. M. Volk, K. A. Walker, and M. Riese, 2015a: Impact of the 2009 major sudden stratospheric warming on the composition of the stratosphere. *Atmospheric Chemistry and Physics*, **15**, 8695–8715, doi: 10.5194/acp-15-8695-2015.

Tao, M. C., P. Konopka, F. Ploeger, M. Riese, R. Müller, and C. M. Volk, 2015b: Impact of stratospheric major warmings and the quasi-biennial oscillation on the variability of stratospheric water vapor. *Geophys. Res. Lett.*, **42**, 4599–4607, doi: 10.1002/2015GL064443.

Ueyama, R., and J. M. Wallace, 2010: To what extent does high-latitude wave forcing drive tropical upwelling in the Brewer-Dobson circulation? *J. Atmos. Sci.*, **67**, 1232–1246, doi: 10.1175/2009JAS3216.1.

Ueyama, R., E. P. Gerber, J. M. Wallace, and D. M. Frierson, 2013: The role of high-latitude waves in the intraseasonal to seasonal variability of tropical upwelling in the Brewer-Dobson circulation. *J. Atmos. Sci.*, **70**, 1631–1648, doi: 10.1175/JAS-D-12-0174.1.

Xie, F., J. Li, W. Tian, J. Feng, and Y. Huo, 2012: Signals of El Niño Modoki in the tropical tropopause layer and stratosphere. *Atmospheric Chemistry and Physics*, **12**, 5259–5273, doi: 10.5194/acp-12-5259-2012.

Xie, F., J. P. Li, W. S. Tian, J. K. Zhang, and C. Sun, 2014: The relative impacts of El Niño Modoki, Canonical El Niño, and QBO on tropical ozone changes since the 1980s. *Environmental Research Letters*, **9**, 064020, doi: 10.1088/1748-9326/9/6/064020.